Asynchronism Induces Second Order Phase Transitions in Elementary Cellular Automata

Nazim A. Fatès

Asynchronism Induces Second Order Phase Transitions in Elementary Cellular Automata

Nazim Fatès

Nazim.Fates@loria.fr

LORIA – INRIA Nancy Grand-Est

Campus Scientifique B.P. 239

54 506 Vandoeuvre-lès-Nancy, France.

February 13, 2008

Abstract

Cellular automata are widely used to model natural or artificial systems. Classically they are run with perfect synchrony, *i.e.*, the local rule is applied to each cell at each time step. A possible modification of the updating scheme consists in applying the rule with a fixed probability, called the synchrony rate. For some particular rules, varying the synchrony rate continuously produces a qualitative change in the behaviour of the cellular automaton. We investigate the nature of this change of behaviour using Monte-Carlo simulations. We show that this phenomenon is a second-order phase transition, which we characterise more specifically as belonging to the directed percolation or to the parity conservation universality classes studied in statistical physics.

keywords: asynchronous cellular automata, stochastic process, discrete dynamical systems, directed percolation, parity conservation, phase transitions, universality class, power laws

Foreword: In this article, we only present a limited set of plots showing our numerical experimentation. The complete set of graphs can be accessed at:
http://www.loria.fr/~fates/Percolation/results.html
The simulations were obtained with the FiatLux CA simulator [9].

1

1   Introduction

With the increase of computing power, cellular automata (CA) are becoming a popular tool used to simulate various real-world systems. While early research was mainly concerned with the study of logical properties of abstract models [24], many efforts now focus on using CA which closely mimic natural or artificial phenomena.

Our research aims at studying the robustness of cellular automata to asynchronous updating, *i.e.*, at evaluating to which extent a small modification of their updating scheme may perturb their behaviour. To tackle this problem, we propose to study not only a single model but a *family* of models, where the members are obtained by varying the updating scheme [10] and keeping the local rule constant. One simple way of producing such variations is to consider the so called α-*asynchronous dynamics* [14], in which each cell updates its state with probability α, the *synchrony rate*, independently at each time step.

To our knowledge, the problem of comparing the behaviour of synchronous versus asynchronous CA was first addressed by means of simulation in [6], with a qualitative evaluation of the changes. Other experimental studies followed showing that the updating scheme was indeed a key point to study [3, 31, 29]. On the theoretical side, few results have been obtained so far: the independence on the order of update history was studied in [15, 23], existence of stationary distributions for infinite systems was studied in [21] and a first classification based on the convergence time was proposed in [13, 14].

The α-asynchronous updating was studied experimentally [12] and it was shown that the 256 Elementary Cellular Automata (ECA) produced various qualitative responses to asynchronism. We were surprised to observe that, in some cases, a small variation of the synchrony rate α could trigger a qualitative change of behaviour. The present work is devoted to understanding these transitions with an experimental approach. We extend the first investigations presented in [11], examining a larger set of rules with an improved precision.

In [12], we conjectured that the origin of the qualitative change of behaviour was a phase transition that belonged to the universality class of *directed percolation* (see below). We emphasise that this hypothesis was mainly supported by the visual observation of the space-time diagrams produced near the critical point. The purpose of this article is to investigate this hypothesis numerically with large Monte-Carlo simulations.

2   First observations

This section introduces formal notations and presents a first set of simple experiments.

2.1 Formal definitions of the model

Let a ring of n cells be indexed by $\mathcal{L} = \mathbb{Z}/n\mathbb{Z}$; a *configuration* is an assignment of state, 0 or 1, to each element of $\mathcal{L}$; the space of configurations is $\{0,1\}^{\mathcal{L}}$. The *density* of a configuration is the ratio of cells in state 1 over the configuration size n. The *kinks density* is the ratio of the number of 01 or 10 patterns over the size of the configuration n. An *Elementary Cellular Automaton* (ECA) is described by a function $f : \{0,1\}^3 \rightarrow \{0,1\}$ called the *local rule*. ECA are indexed according to Wolfram's usual notation [32].

We define the α-*asynchronous updating scheme* as the operation that consists in applying the local rule f with a probability α or keeping the same state with a probability $1 - \alpha$, independently for each cell. This updating scheme defines a probabilistic global rule which operates on the random configurations $(x^t)_{t \in \mathbb{N}}$ according to:

$$\forall i \in \mathcal{L}, \ x_i^{t+1} = \begin{cases} f(x_{i-1}^t, x_i^t, x_{i+1}^t) & \text{with probability } \alpha \\ x_i^t & \text{with probability } 1 - \alpha \end{cases}$$

By taking $\alpha = 1$, we fall back on the classical synchronous case and as α is decreased, the update rule becomes more asynchronous while the effect of an update remains unchanged. For $0 < \alpha < 1$, x^t is a random configuration that depends on the sequence of cells that are updated at each time step.

2.2 Selecting the Rules to Study

In our first work [12], we experimentally detected a first set of rules that showed a qualitative change of behaviour when α was varied continuously. We re-examined this change of behaviour for the 88 Minimal Representative ECA in more details. For each rule, we arbitrarily fixed the ring size to $n = 10\,000$ and we varied α with an increment of 1% from 0.02 to 1. For each α, we started from a uniform random initial configuration and we measured the evolution of the density during $10\,000/\alpha$ steps, putting a limit of $100\,000$ steps for $\alpha < 0.1$. We extracted the average over the second half of the sample, the first half being used as a transient period to ensure that the system was stabilised. This average density can be considered as an estimate of the *stationary density*, *i.e.*, the limit density that would be reached if the system size and the transient time grew to infinity.

Figure 1 shows the estimated stationary density (or kinks density) versus α for ECA 6, 50, and 178 and Figure 2 shows how the variation of α affects the space-time diagrams these rules. We observe that for ECA 6 and 50 (respectively ECA 178), a non-zero density (resp. kinks density) corresponds to the existence of stable branching-annihilating patterns and a zero density (resp. kinks density) corresponds to a rapid extinction of these patterns.

Exploring systematically the 88 Minimal Representative ECA, we observed that ECA 18, 26, 58, 106, and 146 all have plots which are similar to ECA 50. Their behaviour is compatible with a second order phase transition: there exists
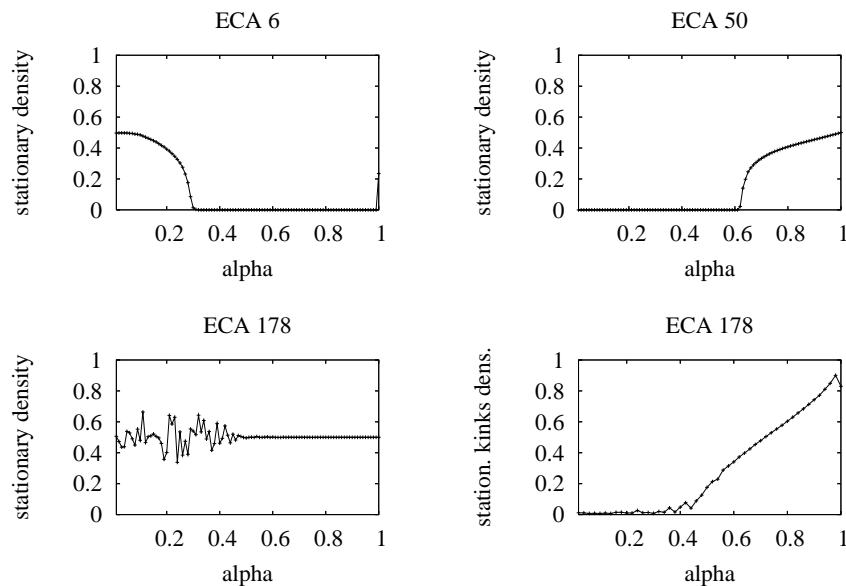
Figure 1: (top) Stationary density versus synchrony rate for ECA 6 (left) and ECA 50 (right). (bottom) ECA 178 : stationary density (left) and kinks density (right) versus synchrony rate. The discontinuity for ECA 6 and 178 at $\alpha = 1$ is not an artifact.

a critical value of α such that for $\alpha > \alpha_c$, the stationary density is non-zero (the *active* phase) and for $\alpha < \alpha_c$ the stationary density is zero (the *inactive* phase). The curve is continuous and reaches zero with an infinite slope for the critical value α_c. As our hypothesis is that the nature of the phase transition is *directed percolation* (see Section 3.2) with an active phase obtained for *high* values of α, we call these rules the DP_{hi} ECA.

ECA 6, 38 and 134 displayed a similar behaviour but what is more surprising is that their phase transition is in an "inversed" pattern: the active phase is obtained for *small* values of α, the inactive phase for large values of α. We call these rules the DP_{low} ECA.

The case of ECA 178 is also peculiar since the density curve is stable for large values of α but does not stabilise value for small values of α. This indicates that, for this particular rule, the choice of measuring density is not suitable. Instead, if we examine the variation of the *kinks* density, we obtain a smooth curve with a discontinuity compatible with a second order phase transition. We call this rule the DP_2 ECA. The choice of this name is justified in the next section.
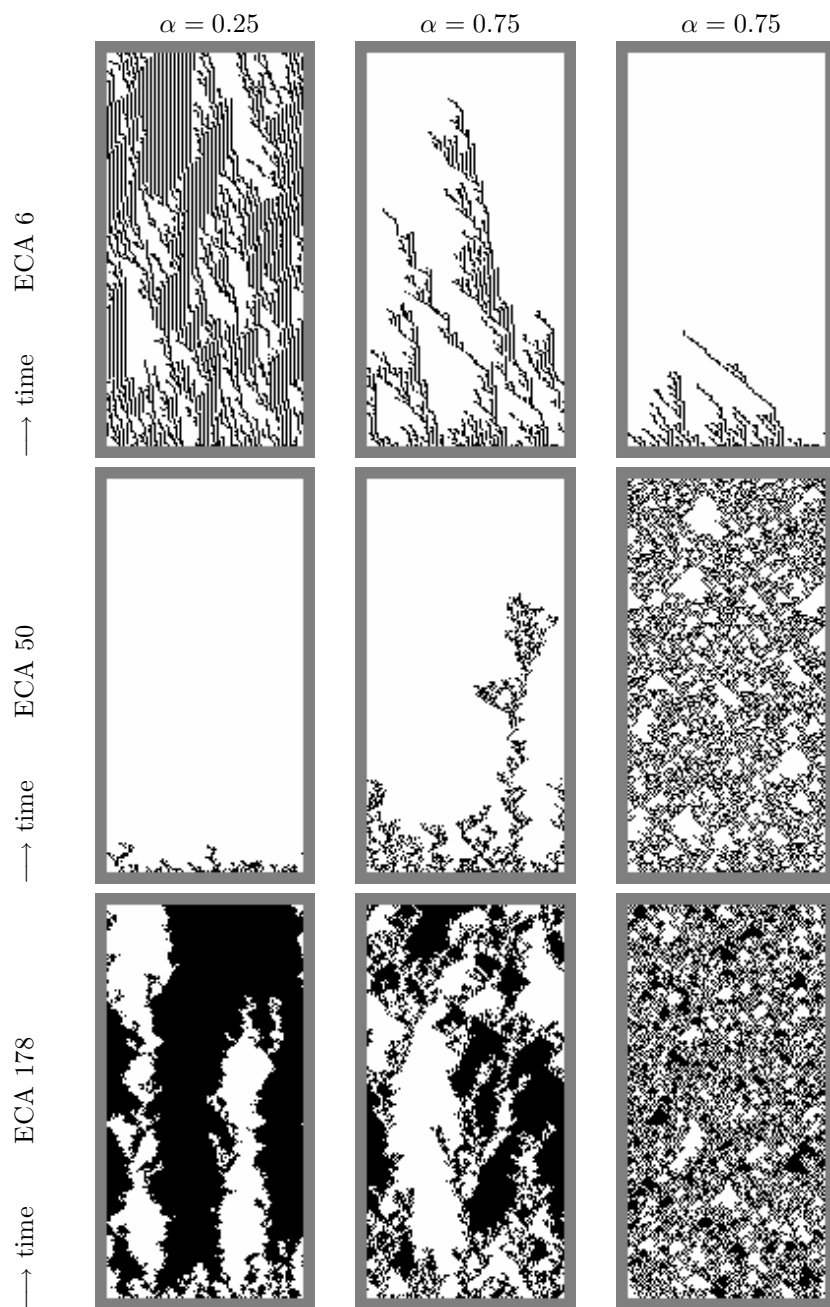
4

Figure 2: Space time diagrams for ECA 6 (top), ECA 50 (middle) and ECA 178 (bottom).Synchrony rate is varied : $\alpha = 0.25$ (left), $\alpha = 0.50$ (middle), $\alpha = 0.75$ (right).Time goes from bottom to top; the time factor is rescaled by a factor $1/\alpha$(i.e., for $\alpha = 0.25$ only time steps that are multiples of 4 are displayed).

3 Phase Transitions

In this section, we present a short review of works related to asynchronous or probabilistic cellular automata and second order phase transitions.

3.1 Universality classes

Many physical or numerical systems exhibit critical phenomena: a continuous change in the value of a control parameter may produce a discontinuous response at the macroscopic level. It is remarkable that near the critical transition, the laws governing the evolution of such systems are generally power laws (see below). In short, one may understand the origin of these power laws from the fact that near the transition point, the system has a self-similar fractal structure and no typical spatial wavelength. An important property is that the same exponents of the power laws, the *critical exponents*, may be found for different models that do not necessarily share the same definitions at the microscopic level.

The collection of all models that are described by the same set of critical exponents is called a *universality class*. Looking at the space-time diagrams produced by the asynchronous ECA, we originally found similarities with the patterns produced by couple map lattices used in hydrodynamics [1]. These similarities lead us to identify our phase transition as possibly belonging to the *directed percolation* (DP) universality class [12].

It is beyond the scope of this paper to list all the models that belong to the directed percolation universality class and we refer to [17, 26] for a review. As far as cellular automata are concerned, directed percolation was observed in various problems. To our knowledge, the first CA that was shown to exhibit DP is the Domany-Kinzel cellular automaton [20, 8]. This model is a tunable probabilistic CA that has the ability to display two different transitions depending on the tuning of its parameters. Various other models involving probabilistic CA were also shown to exhibit DP phenomena (*e.g.*, [27, 28]).

Directed percolation was also identified in problems involving synchronisation of two instances of cellular automata (*e.g.*, [16, 30]). To our knowledge, the only example of directed percolation induced by asynchronism was given by Blok and Bergersen for the famous Game of Life [4]. The protocol they used to identify the universality class of the phase transition relied on the measure of a single critical exponent, the β exponent (see below).

3.2 Directed Percolation

Percolation problems are studied in the fields of discrete mathematics and statistical physics. They were initially motivated by the need to model situations in which a fluid evolves into a porous random medium [5]. In the classical problem of *isotropic percolation*, the porous medium is modelled by a regular infinite two-dimensional square lattice. The nodes of the lattice, or *sites*, can be either *open* (with probability q) or *closed* (with probability $1 - q$) ; the links between
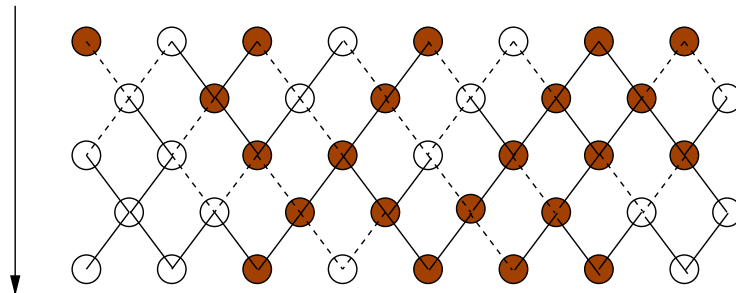
Figure 3: Example of directed bond percolation: filled circles are wet sites, empty circles represent dry sites ; solid (resp. dashed) represent open (resp. closed) bounds. The links can be open with a probablity p. The problem is to determine the critical value p_c for which the size of the clusters of wet sites diverges.

the sites, or *bonds* can also be either *open* (with probability p) or *closed* (with probability $1 - p$). Starting from an initial set of *wet* sites, the question is to determine the set of sites that will also be *wet* if the liquid flows into open sites and open bonds. The sets of all wet sites connected through closed bonds and sites is called a *cluster*.

If we set $q = 1$ (respectively $p = 1$), we have the isotropic *bond* (resp. *site*) *percolation*. For the isotropic bond percolation problem, the average cluster size diverges for the critical value $p_c = 1/2$: we say that the fluids *percolates* through the medium. *Directed* bond percolation is a non-isotropic variant of the previous model in which links are oriented according to a particular direction (see Figure 3). This models situations in which the fluid can go only in one direction, for example when submitted to gravity.

We can also formulate directed percolation as a probabilistic dynamical system: in this case, time plays the role of the non-isotropic dimension. More formally, if we represent the state of a site $i \in \mathbb{N}$ at time t by $s_i^t \in \{0, 1\}$ (dry or wet site), starting from an initial condition s^0, the states of sites are updated according to the simple rule [17]:

$$s_i^{t+1} = \begin{cases} 1 & \text{if } [s_{i-1}^t = 1 \text{ and } \mathcal{L}_i^t(p) = 1] \text{ or } [s_{i+1}^t = 1 \text{ and } \mathcal{R}_i^t(p) = 1] \\ 0 & \text{otherwise} \end{cases}$$

where $(\mathcal{L}_i^t)$ and $(\mathcal{R}_i^t)$ are i.i.d. Bernoulli random variables ; they model the probability for the left or right bond to cell (i, t) to be open or closed.

Theory and observations predict that for an *infinite* lattice and for a fixed value of p, if we start from an initial configuration with all sites in wet state, the density of wet sites $d(p, t)$ evolves to a positive limit for $p > p_c$ and to a zero limit for $p \leq p_c$ [17]. More precisely, if we denote by $d_\infty(p)$ the infinite time limit of $d(p, t)$, for $p > p_c$, near the critical point ($p \to p_c$), the asymptotic

density d_∞ diverges from zero by following a power law:

$$d_\infty(p) \sim (p - p_c)^\beta$$

Note that as we have $\beta < 1$, the right derivative of $d_\infty(p)$ has an infinite value at the critical point. This explains why the transition is experimentally seen as "abrupt" when p is varied smoothly. At the critical point $p = p_c$, the density vanishes to zero $d_\infty(p_c) = 0$ and the decrease follows a power law:

$$d(p_c, t) \sim t^{-\delta}$$

The values of the two critical exponents $\delta = 0.1595$ and $\beta = 0.2765$ are known by numerical simulations (the values are given here with four digits, see [17] for a better precision). Determining their values analytically is difficult and it is so far an open problem to know whether these exponents are rational numbers. There are also other critical exponents that can be used to identify a universality class but we choose here to focus only on the measure of β and δ exponents (following [25, 16] for instance).

3.3 The PC-DP$_2$ class

In the case where the local rule has two *symmetric states*, it is generally observed that the phase transition is either in the $\mathbb{Z}_2$-*symmetric directed percolation* (DP$_2$) class or in the *parity-conserving* class (PC). Again, we refer to [17, 26] for a detailed description of these two universality classes, their similarities and differences. In short, the PC class appears when one considers models with branching-annihilating random walks with an *even* number of offspring (*e.g.*, [19]). The DP$_2$ class is observed with models that introduce two *symmetric* states, as it is the case for ECA 178.

It is well known that the two classes coincide for dimension 1 and differ for higher dimensions. An intuitive reason for this surprising property is indicated by Hinrichsen [17] : "active sites of PC models in $d \geq 2$ dimensions can be considered as branching-annihilating *walkers*, whereas DP$_2$ models describe the dynamics of branching annihilating *interfaces* between oppositely oriented inactive domains". From the observation of space-time diagrams of ECA 178 and by analogy with other models, we conjectured that the phase transition of this rule belonged to the DP$_2$ universality class [10].

3.4 Hypotheses to test

The phase transition theory stipulates that there should be two macroscopic parameters, respectively called *the control parameter* and *the order parameter*, that satisfy the power laws near the critical point. For the sake of simplicity, we use the synchrony rate α as a control parameter and the density d as an order parameter. However, note that other possibilities may also be examined, for example in [4] the authors also use the *activity* (*i.e.*, the ratio of cells in an unstable state) as an order parameter. For the nine DP ECA identified in Section 2, we thus expect to measure:

- $d(\alpha_{\mathrm{c}}, t) \sim t^{-\delta}$ at the critical point,

- $d_\infty(\alpha) \sim {\Delta_\alpha}^\beta$ near the critical point, for the active phase,

with $\Delta_\alpha = \alpha - \alpha_{\mathrm{c}}$ for the $\mathsf{DP}_{\mathrm{hi}}$ ECA and $\Delta_\alpha = \alpha_{\mathrm{c}} - \alpha$ for the $\mathsf{DP}_{\mathrm{low}}$ ECA. For the DP_2 rule ECA 178, we take the kinks density as an order parameter. By contrast with the DP universality class the exponents of the PC and DP_2 classes are known analytically. In particular we have $\delta_{\mathrm{DP2}} = 2/7$ for two-dimensional lattices. (Recall that space and time play a role analogous to the two dimensions of the grid in the original directed percolation problem.)

3.5 Protocol and Measures

The measure of the DP critical exponents is a delicate operation that generally requires a large amount of computation time. The main difficulty resides in avoiding systematic errors when obtaining statistical data near the transition point. Authors have been mislead by their measures and concluded that a phase transition phenomenon was not in the DP universality class, which has later been proved wrong by using a different protocol and more precise measures [18, 16]. In order to limit the influence of systematic errors, we take the two-step protocol used in [16]:

- We measure the critical synchrony rate α_{c} by varying α until we reach the best approximation of a power law decay for the density. This first experiment also allows us to measure the critical exponent δ.

- We measure the stationary density d_∞ as a function of $|\alpha - \alpha_{\mathrm{c}}|$ and then fit a power law in order to calculate β.

Note that these two steps are not independent since the second operation uses the previously computed value of α_{c}.

The other main concern is to evaluate the influence of finite size effects and metastability. In the active phase, finite DP systems are in an *out-of-equilibrium* state. This means that although infinite-size systems have a stable probability measure for the distribution of states, the finite-size systems used in the simulations may attain the absorbing state even if they are in the active phase. There exist many techniques to handle this problem, for example adding a small amount of noise to prevent the system from staying indefinitely in the absorbing state. In this work we choose to use large size lattices and verify experimentally that the results are not influenced by the trajectories that touch the absorbing state (here $\mathsf{0}^{\mathcal{L}}$).

We will present the curves for ECA 50 while only numerical data will be given for the other DP ECA. Indeed, rule 50 can be written in the rather simple form:

$$\forall (a, b, c) \in \{\mathsf{0}, \mathsf{1}\}^3, \ f(a, b, c) = \begin{cases} 1 - b & \text{if } (a, b, c) \neq (\mathsf{0}, \mathsf{0}, \mathsf{0}) \\ \mathsf{0} & \text{if } (a, b, c) = (\mathsf{0}, \mathsf{0}, \mathsf{0}) \end{cases}$$

9

It is possible to see this rule as a one dimensional version of an "epidemic" rule: a healthy cell (state 0) gets infected (state 1) if at least one of its neighbour is infected ; once it is infected, it becomes healthy at the next update of the cell.

4 Finding the Critical Synchrony Rate α_c

Following our protocol, we estimate the critical point by determining the change of convexity of the density curves in a log-log plot. The concave function characterises the *active* phase as the asymptotic density evolves towards a non-zero value ; the convex function corresponds to the *inactive* phase as the density evolves to zero with an exponential decay.

For ECA 50, the previous experiment (Figure 1) allowed us to locate the critical synchrony rate around $\alpha_c \sim 0.62$. Figure 4 shows the temporal decay of the density curve in a log-log plot, with α varied by increments of 10^{-3} around 0.62. The change of convexity is found between 0.627 and 0.629. The curves are obtained by averaging the data on $N_\mathrm{s} = 100$ runs obtained on a ring size $n = 20\,000$ and a sampling time of $T = 200\,000$ steps.

To improve our estimate of α_c to a precision of 10^{-4}, we extended the sampling time to $T = 10^7$ and we increased the ring size to $n = 40\,000$. Figure 4 shows the two values $\alpha_\mathrm{c}^- = 0.6381$ and $\alpha_\mathrm{c}^+ = 0.6383$ for which we observed the change of convexity. We repeated the same type of progressive approximations of α_c for all the DP ECA. It was always possible to observe the change of convexity when varying α with an increment of 10^{-4}. However, the sampling time T, the ring size n and the number of samples N_s had to be adapted to each ECA to ensure a good stability of the measures (see below). The values of the estimated critical synchrony rates are reported in Table 1.

4.1 Measurement of δ

The value of δ is given at the critical point by the slope of the density curve in a log-log scale (see Section 3.4). We report in Table 1 the time interval $[T_\mathrm{min}, T_\mathrm{max}]$ used to compute δ. The lower limit T_min is obtained by a rough estimate of the maximum transient time needed for the system to enter into the power law regime. The upper limit of the interval T_max corresponds to the minimum time for which the deviation from a power law decay becomes visible for the curves α_c^- and α_c^+ that show the change of convexity.

We bring to the reader's attention the fact that it is a difficult problem to estimate the error on δ. Indeed, besides the influence of noise, the value depends on the time interval $[T_\mathrm{min}, T_\mathrm{max}]$ used to perform the fit. There is to our knowledge no general method for choosing this time interval. To estimate the error on δ, we computed the different values obtained when varying α to α_c^- and α_c^+ and by varying T_min and T_max by a factor 2. Numerical values of δ are reported in Table 1 for comparison with δ_DP. Given our estimations of uncertainty, the results show good agreement with $\delta_\mathrm{DP} = 0.1595$.
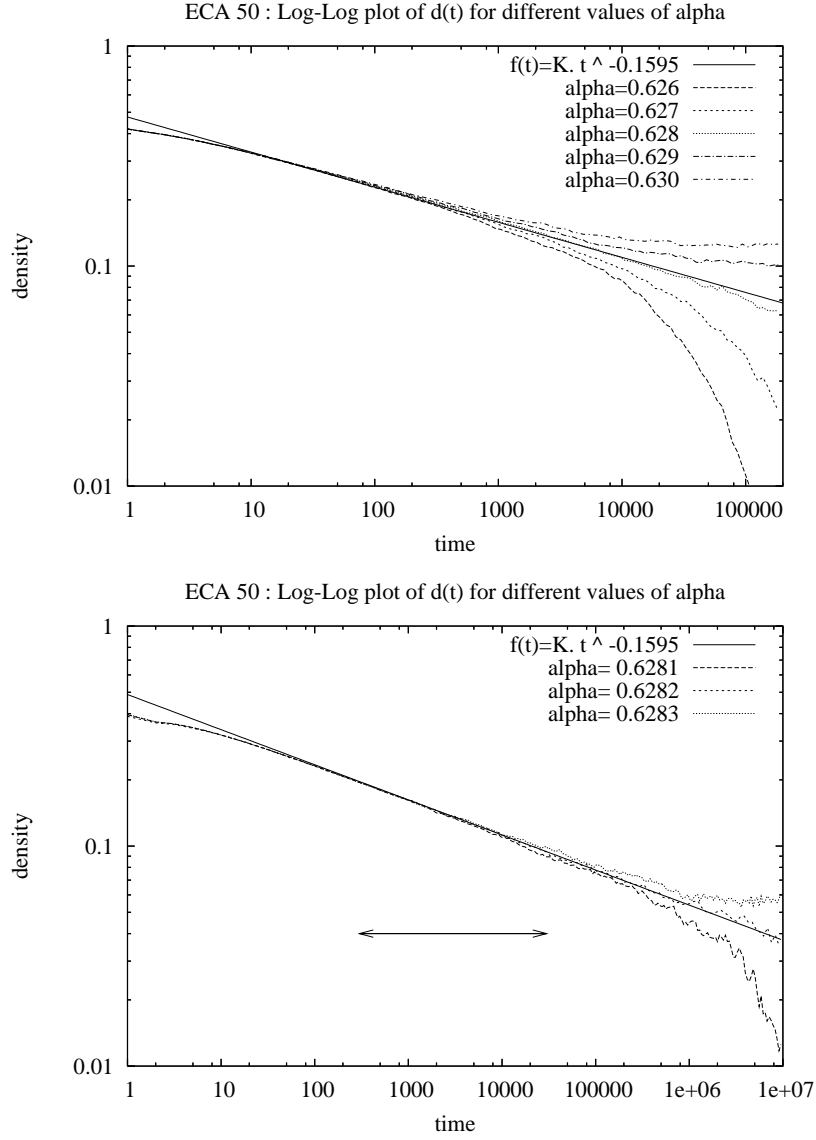
Figure 4: ECA 50: Determination of the critical synchrony rate α_c. The straight line has slope $-\delta_{\mathrm{DP}} = -0.1595$ and is plotted for reference. (above) Averages obtained on $N_s = 100$ runs, ring size $n = 20\,000$, sampling time $T = 2 \times 10^5$. (below) Averages obtained on $N_s = 50$ runs and ring size $n = 40\,000$, sampling time $T = 10^7$. The arrow indicates the interval $[T_{\min}, T_{\max}]$ used to perform the fit to measure δ.

4.2 Stability of the measures

An important question is to determine whether the visual estimations of the changes of convexity are satisfying and stable. A simple method to verify this is to estimate numerically the "linearity" of the density curves (in a log-log representation). For the sake of simplicity, we used the root mean square error of the fits as a linearity estimator. For example, for ECA 50, fitting a power law in the time interval $[300, 30\,000]$ for $\alpha_c^- = 0.6181$, $\alpha_c = 0.6282$, $\alpha_c^+ = 0.6283$ gives an error of 0.16, 0.10, 0.13 (dimensionless units), respectively, which confirms that the "most linear" curve is obtained with α_c.

The other point of care concerns the measurement of the critical exponent δ. Recall that we needed to distinguish the "power law" part $[T_{\min}, T_{\max}]$ of the density curve and the "departure from power law" $[T_{\max}, \infty[$, which can be convex or concave. To which extent does δ depend on the choice of $T_{\min}$ and $T_{\max}$? Firstly, let us note that the length of transient time interval $[0, T_{\min}]$ only depends on the ECA considered while the length of the "power law" part of the curve $[T_{\min}, T_{\max}]$ is a function of the distance to the critical point $|\alpha - \alpha_c|$: the smaller this value, the longer the system follows the power law predictions. This means that the values of $T_{\max}$ depend heavily on our choice of increment on α. In our experiment, we found out that it was necessary to take an increment on α as small as 10^{-4} to ensure that the time interval $[T_{\min}, T_{\max}]$ was large enough to measure δ with a good precision.

Secondly, recall that as we use finite size lattices, the system is metastable: it eventually reaches the absorbing state $0^{\mathcal{L}}$, whatever the value of α. In order to infer the infinite-size limit from the simulations obtained on *finite* systems, we need to take n large enough to ensure that the trajectories do not that reach the absorbing state. For all the DP ECA but ECA 18, we used $n = 40\,000$ to satisfy this condition ; for ECA 18, it was necessary to take $n = 80\,000$ to prevent the system from reaching the absorbing state.

Finally, the case of ECA 134 also needs to be underlined as its density curve has many inflexion points, which makes it harder to measure α_c and δ.

5 Determination of β

In this second part of the experiment, we measure the β critical exponent by estimating the stationary density as a function of $\Delta_\alpha = |\alpha - \alpha_c|$.

5.1 Measurement of β

There are two different possibilities for varying Δ_α: some authors use linear variation (*e.g.*, [4]) while others use an exponential variation. As we expect the curve d_∞ versus Δ_α to be linear in a log-log plot, we varied Δ_α with an exponential increment of $\sqrt{2}$ from 8×10^{-4} to 0.512, which allowed us to obtain equally spaced points in the log-log scale. Figure 5 shows the evolution of the density versus time for different values of Δ_α.
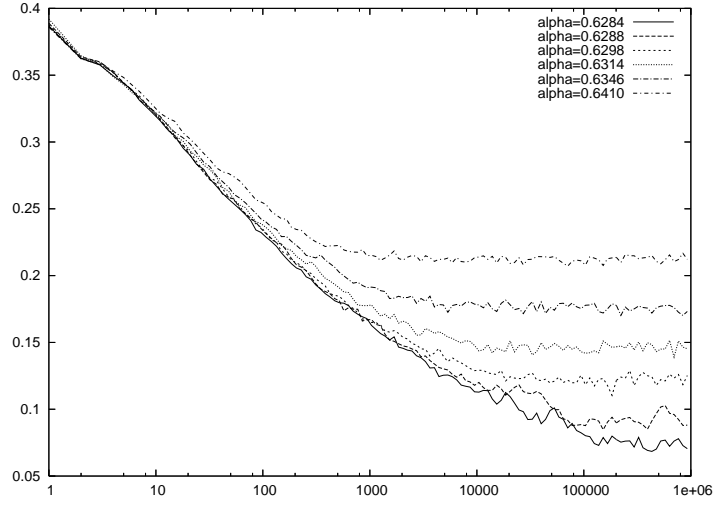
Figure 5: ECA 50: Evolution of the density versus time for $\alpha > \alpha_c = 0.6282$. The ring size is $n = 2 \times 10^4$; averages use $N_s = 10$ runs with a sampling time $T = 10^6$.
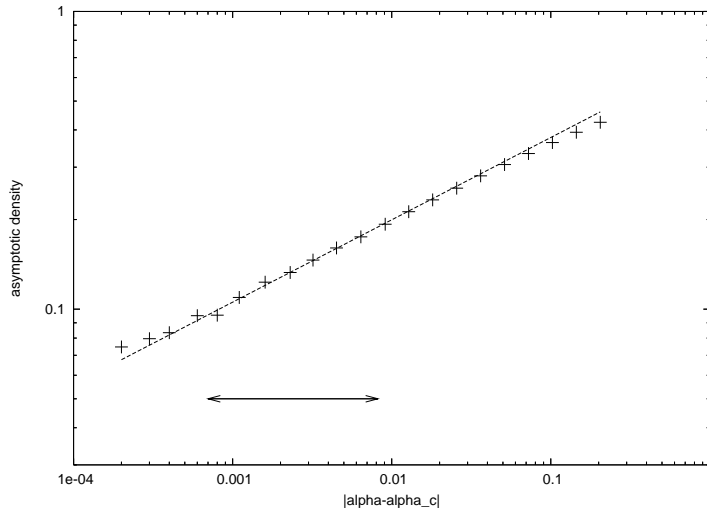

Figure 6: ECA 50: Determination of the critical exponent β using the time decay properties (see text). The straight line shows theoretical prediction and has slope: $\beta_{DP} = 0.2765$. Note that both x and y axis are displayed in logarithmic scale. The arrow shows the fit interval used to calculate the β exponent.

13

Following the observations of the previous experiment, we estimated the stationary density $d_\infty(\alpha)$ by measuring $d(t)$ during $T = 10^6$ steps and by taking the average of d on the time interval $[T/2, T]$. To limit the influence of the noise, we repeated $N_s = 10$ times the measure and took the average value. Note that even though T can be adjusted as a function of Δ_α, we prefer to take a fixed value for T for the sake of simplicity. This value was adjusted for the *minimal* value of Δ_α, which makes it a priori suitable for larger values of Δ_α (see Figure 5).

Figure 6 shows the estimated values of d_∞ as a function of Δ_α. The visual comparison with the expected plot shows a good agreement with the predicted value of DP. For each ECA, we took $t \in [20 \times 10^{-4}, 20 \times 10^{-3}]$ as a fit interval. The estimated values of β are reported in Table 1 ; as for the δ exponent, they show good agreement with the DP prediction $\beta_{DP} \sim 0.276$.

5.2 Stability of the measures

To which extent do these measures depend on the setting of the parameters of the experiment? We observe on Figure 6 that the linear part of the density curve is limited by two competing phenomena. Note that the small values of Δ_α are always overestimated. This can be explained by remarking that, near criticality the stationary density vanishes as: $d_\infty(\alpha) \sim \Delta_\alpha{}^\beta$. Note that we also have $d \sim t^{-\delta}$ near criticality, which implies that the time needed to get close to the stationary density increases exponentially with $1/\Delta_\alpha$. This phenomenon, known as the *critical slowing down* (*e.g.*, [17]), limits the measurement of the stationary density for small values of Δ_α.

For the higher values of Δ_α, the system "saturates" and no longer follows a power law (a density can not be higher than 1). The deviation from the power law is a phenomenon that is predicted by theory and that can be studied for its own interest. We prefer here to restrict our measures to the linear part of the curve. However, some authors advocate that the study of the deviations from the power law significantly improves the determination of a universality class [22]. To estimate the error on β, we measured how its value changed when α_c was varied in the interval $[\alpha_c^-, \alpha_c^+]$ and when the fit interval was changed to $[30 \times 10^{-4}, 30 \times 10^{-3}]$. We noticed that the error was mainly due to the uncertainty on α_c and had an order of magnitude of 10^{-2}.

6 The case of ECA 178

For ECA 178, we repeated the protocol described above using the the kinks density instead of the density as an order parameter. Our best results were obtained with $n = 80\,000$, $T = 10^8$ and $N_s = 50$: we located a change of convexity between $\alpha_c^- = 0.409$ and $\alpha_c^+ = 0.411$. However, by contrast with the previous DP ECA, this change of convexity was much more difficult to observe. This well-known difference is explained by the algebraic decay of the order parameter in PC or DP_2 models. This produces straight lines in a log-log

Table 1: Numerical Results for the DP and DP$_2$ rules : the digit between parentheses is uncertainty on the last digit. Compare with $\delta_{DP} = 0.1595$, $\delta_{DP2} = 0.2856$ and $\beta_{DP} = 0.276$.

ECA	$\tilde{\alpha}_c$	δ	T_{min}	T_{max}	β
6	0.2825 (1)	0.160 (3)	1×10^3	3×10^5	0.27 (1)
18	0.71385 (5)	0.157 (3)	5×10^1	2×10^4	0.27 (1)
26	0.47485 (5)	0.159 (1)	1×10^3	2×10^5	0.27 (1)
38	0.04085 (5)	0.160 (4)	2×10^4	4×10^5	0.27 (1)
50	0.6282 (1)	0.158 (3)	3×10^2	3×10^4	0.27 (1)
58	0.3398 (1)	0.161 (4)	1×10^3	1×10^5	0.28 (2)
106	0.8146 (1)	0.157 (2)	5×10^2	3×10^5	0.28 (1)
134	0.0821 (2)	0.161 (5)	2×10^4	2×10^6	0.26 (3)
146	0.6751 (1)	0.158 (3)	5×10^1	1×10^5	0.27 (2)
178	0.410 (1)	0.286 (4)	1×10^2	2×10^5	? (?)

scale which makes changes of convexity less visible than the exponential decay observed for the DP ECA. This explains why it is difficult to estimate α_c with a better precision despite using a long computation time.

In the time interval $[100, 20\,000]$, the fit for the curve $\alpha_c = 0.410$ gives a slope of $\delta = 0.2860$, which is close to the predicted value $\delta_{DP2} \sim 0.2856$. To estimate the error on δ, we repeated the fit with the same time interval, but with the curves obtained with α_c^- and α_c^+. We found that δ varied less than 4×10^{-3}. As the precision on δ is good while the precision on α_c is relatively poor for this rule, we did not measure the critical exponent β. A possible way of improving our measure of the critical point α_c consists in using a different experimental protocol, for example measuring the "dynamical" exponents obtained by starting from an initial condition close to the absorbing state.

7 Discussion

We experimentally investigated how qualitative changes of behaviour were triggered by gradual variations of the synchrony rate in asynchronous cellular automata. The results show good evidence that these phenomena are second order phase transitions which belong to the directed percolation (DP) and parity conservation (PC- DP$_2$) universality classes.

From a practical point of view, the main limitation for identifying the phase transitions was the huge amount of computation time required for measuring the critical exponents : for each ECA, we used approximately 10^{15} computations of the local rule in order to determine these exponents with two or three digits. This task represented several months of calculus with several personal computers. It calls for further studies on how to improve the computation process (*e.g.*, the generation of random numbers) or on how to take advantage of the use of massively parallel computing devices.

15

7.1 The origin of phase transitions

The observation of the synchronous behaviour of the rules we studied indicate that there is certainly no straightforward relation with the existing classifications. For example, ECA 50 is "periodic" (or Wolfram class II) while ECA 18 is "chaotic" (or Wolfram class III). This indicates that some particular asynchronous cellular models obey the *same* macroscopic laws near their transition points despite of having different definitions at the microscopic cell-scale. In other words, the asynchronous updating of cellular systems unveils another type of complexity which still needs to be understood.

A first path for discussing these results is to consider the famous conjecture by Janssen and Grassberger (*e.g.*, see [17] for a short presentation). It states that a model should belong to the DP universality class *if* it satisfies the following criteria: **(a)** the model displays a continuous phase transition from a fluctuating active phase to a *unique* absorbing state, **(b)** it is possible to characterise the phase transition by a positive one-component order parameter, **(c)** the dynamics of the model is defined by short-range process, and **(d)** there exists no additional symmetries or quenched randomness (*i.e.*, small and stable topological modifications).

For all the DP ECA, we saw that condition **(a)** was fulfilled with $0^{\mathcal{L}}$ as the absorbing state. It is interesting to note that configuration $0^{\mathcal{L}}$ is a fixed point for all the DP rules, but ECA 134 and 146 also have $1^{\mathcal{L}}$ as a fixed point. This confirms that the informal notion of "absorbing state" can not be trivially identified with the fixed point mathematical property. Condition **(b)** was fulfilled by the density or by the kinks density. Condition **(c)** is true by definition of cellular automata.

Analysing condition **(d)** is more interesting since we see a difference between *space* symmetry, which is possessed by ECA 50 for example, and *state* symmetry (*i.e.*, invariance under 0 and 1 exchanging), which is absent for all the DP ECA. This may also explain why ECA 178, which has both symmetries, has a peculiar behaviour and was found in the PC-DP$_2$ universality class. Note that conditions **(b)**, **(c)**, **(d)** can be easily verified but a challenging question consists in explaining why only a small fraction of the 256 ECA also verify condition **(a)** and thus exhibit DP behaviour.

7.2 Perspectives

At this point, it is still an intriguing question to understand the origin of out-of-equilibrium phase transitions in cellular automata, and more generally, in particle systems. The models we exhibited count among the simplest models that display out-of-equilibrium phase transitions. In that respect, they can be used as a good basis for exploring the origin of phase transitions by analytical means or by numerical simulations.

A further step for understanding asynchronous cellular automata is to make a "reduction" between the DP rules, *i.e.*, to show that if one of them exhibits such a phase transition, then the others behave similarly. Another step is to ex-

tend such a reduction to other well-studied systems such as the Domany-Kinzel probabilistic CA [8]. This implies uniting the two types of phase transitions we observed: recall that going from the inactive to active phase was obtained either by *increasing* ($\mathrm{DP_{hi}}$ ECA) or by *decreasing* ($\mathrm{DP_{low}}$ ECA) the control parameter. To our knowledge, it is the first example where these two-way transitions are observed.

A more ambitious possibility for unifying the study of all the DP ECA is to consider the larger set of *probabilistic* elementary cellular automata, which include the α-asynchronous ECA. In this space, which is homeomorphic to $[0,1]^8$, the problem is to determine whether the phase transitions can be explained in terms of crossing of a hypersurface (see also [7]).

Our view is that there exists a wide range of problems that could benefit from the study of cellular systems with out-of-equilibrium phase transitions. For example, in biology, can we explain the trigger of the self-organisation phase in cellular societies by using similar models [12, 2]? In an engineering context, can we use phase transitions to design systems that change their behaviour without any external control ?

References

[1] Pierre Berg, Yves Pomeau, and Monique Dubois. *Des rythmes au chaos*. Odile Jacob, 1994.

[2] Hugues Berry. Nonequilibrium phase transition in a self-activated biological network. *Physical Review E*, 67:031907, 2003.

[3] Hugues Bersini and Vincent Detours. Asynchrony induces stability in cellular automata based models. In Rodney A. Brooks and Pattie Maes, editors, *Proceedings of the 4th International Workshop on the Synthesis and Simulation of Living Systems ArtificialLifeIV*, pages 382–387. MIT Press, July 1994.

[4] Hendrik J. Blok and Birger Bergersen. Synchronous versus asynchronous updating in the "game of life". *Physical Review E*, 59:3876–9, 1999.

[5] S.R. Broadbent and J.M. Hammersley. Percolation processes I. Crystals and mazes. *Proceedings of the Cambridge Philosophical Society*, 53(3):629–641, 1957.

[6] Buvel, R.L. and Ingerson, T.E. Structure in asynchronous cellular automata. *Physica D*, 1:59–68, 1984.

[7] H. Chaté and P. Manneville. Spatio-temporal intermittency in coupled map lattices. *Physica D*, 32:409–422, 1988.

[8] Eytan Domany and Wolfgang Kinzel. Equivalence of cellular automata to Ising models and directed percolation. *Physical Review Letters*, 53:311–314, 1984.

[9] Nazim Fatès. Fiatlux CA simulator in Java. See `http://nazim.fates.free.fr` for downloading.

[10] Nazim Fatès. *Robustesse de la dynamique des systèmes discrets : le cas de l'asynchronisme dans les automates cellulaires*. PhD thesis, École normale supérieure de Lyon, 2004.

[11] Nazim Fatès. Directed percolation phenomena in asynchronous elementary cellular automata. In Samira El Yacoubi, Bastien Chopard, and Stephania Bandini, editors, *Proceedings of the 7th International Conference on Cellular Automata for Research and Industry*, volume 4173 of *Lecture Notes in Computer Science*, pages 667–675. Springer, 2006.

[12] Nazim Fatès and Michel Morvan. An experimental study of robustness to asynchronism for elementary cellular automata. *Complex Systems*, 16:1–27, 2005.

[13] Nazim Fatès, Michel Morvan, Nicolas Schabanel, and Eric Thierry. Fully asynchronous behavior of double-quiescent elementary cellular automata. *Theoretical Computer Science*, 362:1–16, 2006.

[14] Nazim Fatès, Damien Regnault, Nicolas Schabanel, and Eric Thierry. Asynchronous behavior of double-quiescent elementary cellular automata. In José R. Correa, Alejandro Hevia, and Marcos A. Kiwi, editors, *Proceedings of LATIN 2006*, volume 3887 of *Lecture Notes in Computer Science*, pages 455–466. Springer, 2006.

[15] Peter Gács. Deterministic computations whose history is independent of the order of asynchronous updating. `http://arXiv.org/abs/cs/0101026`, 2003.

[16] Peter Grassberger. Synchronization of coupled systems with spatiotemporal chaos. *Physical Review E*, 59(3):R2520, March 1999.

[17] Haye Hinrichsen. Nonequilibrium critical phenomena and phase transitions into absorbing states. *Advances in Physics*, 49:815–958, 2000.

[18] Iwan Jensen. Universality class of a one-dimensional cellular automaton. *Physical Review A*, 43(6):3187–3189, 1991.

[19] Iwan Jensen. Critical exponents for branching annihilating random walks with an even number of offspring. *Pysical Review E*, 50(55):3623, 1994.

[20] Wolfgang Kinzel. Directed percolation. In R. Zallen G. Deutscher and J. Adler, editors, *Percolation Structures and Processes*, page 425. Adam Hilger Pub. Co., Bristol, 1983.

[21] Pierre-Yves Louis. *Automates Cellulaires Probabilistes : mesures stationnaires, mesures de Gibbs associées et ergodicité*. PhD thesis, Université des Sciences et Technologies de Lille, September 2002.

18

[22] Sven Lübeck. Universal scaling behavior of non-equilibrium phase transitions. *International Journal of Modern Physics B*, 18(31-32):3977–4118, 2004.

[23] Matthew Macauley, Jon McCammond, and Henning S. Mortveit. Order independence in asynchronous cellular automata. *Journal of Cellular Automata (in press)*, 2008.

[24] Edward F. Moore. Machine models of self-reproduction. *Proceedings of Symposia in Applied Mathematics*, 14:17–33, 1962. (Reprinted in Essays on Cellular Automata, A.W. Burks (ed.), University of Illinois Press, 1970).

[25] Luis G. Morelli and Damian H. Zanette. Synchronization of stochastically coupled cellular automata. *Physical Review E*, pages R8–R11, July 1998.

[26] Géza Ódor. Universality classes in nonequilibrium systems. *Reviews of modern physics*, 76, 2004.

[27] Géza Ódor, Nino Boccara, and György Szabó. Phase transition study of a one-dimensional probabilistic site-exchange cellular automaton. *Physical Review E*, 48(4):3168–3171, 1993.

[28] Géza Ódor and Attila Szolnoki. Directed-percolation conjecture for cellular automata. *Physical Review E*, 53(3):2231–2238, 1996.

[29] Andrea Roli and Franco Zambonelli. Emergence of macro spatial structures in dissipative cellular automata. In *Proc. of ACRI2002: Fifth International Conference on Cellular Automata for Research and Industry*, volume 2493 of *Lecture Notes in Computer Science*, pages 144–155. Springer, 2002.

[30] Jean-Baptiste Rouquier. Coalescing cellular automata. In *Proceedings of ICCS'06*, volume 3993 of *Lecture Notes in Computer Science*, pages 321–328, 2006.

[31] Birgitt Schönfisch and André de Roos. Synchronous and asynchronous updating in cellular automata. *BioSystems*, 51:123–143, 1999.

[32] Stephen Wolfram. Universality and complexity in cellular automata. *Physica D*, 10:1–35, 1984.

8 Acknowledgements